Thermogravimetric-mass spectrometry study of pyrolysis of Botswana-Morupule coal: kinetic parameters determination using iso-conversional and model fitting methods

Kgalalelo P. Kgatlane[1,2] · Sebusi Odisitse[1] · Casper Gate[3] · James Darkwa[2,4] · Isaac N. Beas[2,5]

Abstract

Thermogravimetric-mass spectrometry studies were carried out to determine the evolved gas during the pyrolysis of Morupule coal. Pyrolysis of the three kinds of coal (EM1, WM1 and S3-5) were carried out at various heating rates in an inert atmosphere and temperatures ranging from 25 to 900 °C. Volatile products (H_2, CO, CO_2, H_2O, CH_4) were released in relative intensities, indicating their quantities. Light volatiles such as H_2 (m/z = 2) and H_2O (m/z = 18) dominated the evolved gaseous products, while carbon oxides as CO (m/z = 29) and CO_2 (m/z = 44) and aliphatic hydrocarbon as CH_4 (m/z = 15) were the lesser products. Iso-conversional methods (Friedman and advanced integral Vyazovkin) were applied to calculate the kinetic parameters of the coal. The advanced integral Vyazovkin method was more suitable as it involves more accurate approximations. The mean activation energy calculated from the advanced integral Vyazovkin method was 155–224 kJ/mol.

Keywords Coal · Thermogravimetric mass spectrometry · Pyrolysis · Evolved gas · Kinetics · Activation energy · Model-free methods

Abbreviations
TG   Thermogravimetry
TGA   Thermogravimetry analysis
DTG   Differential thermogravimetry
FWO   Flynn–Wall–Ozawa method
KAS   Kissinger–Akahira–Sunose method

List of symbols
A   The pre-exponential factor (min^{-1})
Eα   The activation energy (kJ/mol)
f(α)   The derivative representation of the reaction model

Extended author information available on the last page of the article

m   Mass of samples m_0 original mass of the sample
m_f Mass after pyrolysis
R   The universal gas constant (8.314 J/mol/K)
R^2 The degree of linear fitting
T   The absolute temperature (°C)
n   Reaction order
k(T)   Reaction rate constant
m/z   Mass to charge ratio
t   Time (s)

Greek letters
β   Heating rate
α   Degree of conversion

Subscripts
i   The stage number in the overall reaction process
j   The number of classical reaction mechanism function

Introduction

The most widely available fossil fuel is coal. Reports show that it will remain accessible long after petroleum and natural gas wells have run dry [1]. It is a significant contribution to fossil fuel energy sources and resources. It is the most important primary energy source for most countrie's power generation and industrial processes and will remain so until at least 2030 [2]. Because coal is comparatively cheaper than other fossil fuels like natural gas and oil, it remains vital in achieving a diverse and balanced energy source for developed and developing economies, providing 26% of global primary energy needs and 41% of global electricity generation [3]. But for coal to be used prudently and avert its associated pollution, it is imperative to understand each country or region's coal for energy generation purposes. Black lignite coals have been widely utilized to generate electricity and industrial steam in Botswana, Mozambique, Zambia, Zimbabwe, and Namibia [4]. Since Botswana has a considerable amount of this domestic energy resource and an existing capacity for coal-based power production, such coals are anticipated to remain a vital energy source for both countries for several decades to come. Coal is one of Botswana's abundant energy resources (200 billion tons) [5]. The Morupule Coal Mine currently serves as the only mine producing coal. The major consumers of the Morupule coal are the Botswana Power Cooperation which uses it to generate electricity throughout the country and Selibe-Phikwe mines which used the coal for smelting copper and nickel when the smelter was in operation.

It is well established that gasification can improve power generation efficiencies from 35% for coal combustion to 45 and 55% [6]. Thus, carbon dioxide emissions into the atmosphere can also be minimized or more easily recovered. In addition, Campoy et al. showed that a suitable combination of temperature and steam results

in greater yields of CO and H_2, calorific value, carbon conversion and gasification efficiency [6].

Keboletse et al. examined the suitability of Morupule coal for gasification technology and found more hydrogen flowing inside the reactor than other combustible gases [7]. CO followed this, while CH_4 was the least produced gas. Gasification kinetics of Morupule coal under atmospheric CO_2 isothermal temperatures of 900–1050 °C in an efficient wire-mesh reactor has been studied by Bikane et al., who found that rates of response of gasification were substantially higher than those reported in the literature, with an activation energy of 320 kJ/mol as well as a pre-exponential factor of the order of 1010 s^{-1} [8]. A similar study of Morupule coal with thermogravimetry by Tabbiruka et al. found an average heat of coal combustion of 27.3 kJ/g, with a substantial amount of ashes after combustion [9]. Neither of the above two studies on Morupule coal is on pyrolysis, but because most of the use of coal involves pyrolysis, several researchers have studied pyrolysis kinetics of different coals in the world [10, 11] but not Botswana coal.

We have, thus, used the thermogravimetric-mass spectrometric (TG-MS) technique to explore the pyrolysis characteristics as well as the kinetics of Botswana's black lignite coal. The results contribute to a better understanding of Botswana's black lignite coal's combustion features and accurate design of pyrolysis systems and the optimization of operating conditions when used in Botswana and in countries that import coal from Botswana.

Materials and methods

Thermogravimetric analysis

The three coal samples utilized in this investigation were collected from the Morupule mine in Palapye (Botswana) from different mining sites [12]. The samples were dried and pulverized to millimeter size with particle sizes of (0.6, 0.850, 1.0, 1.18 and 2.0 mm). About 15 mg of each sample was heated in a Mettler Toledo Thermogravimetric Analyzer (TGA/DSC3+) coupled with a quadrupole Hidden Analytical Mass Spectrometry (Hiden HPR-20 EGA) from 25 to 900 °C using a variety of heating rates (5, 10, 15, 20, 25 °C) using argon flow rate of 40 mL/min to sweep out the volatile products. Each experiment was run three times to ensure reproducibility. Thermal characteristics, model fitting kinetics and isoconversional methods of three different coal samples were used in this study. The gas released from the thermogravimetry is connected to the MS via a heated line using a standard flow capillary-coated quartz tube operated in vacuum, where the MS detects the characteristic fragment ion intensities of the volatiles based on their mass-to-charge ratios. The MS was set to detect gas products in the mass range 1–300. Prior to experiments, the TGA/DSC3+'s temperature readings were calibrated using an Indium reference standard. Data analysis was performed using THINKS, a free, open-source thermokinetic software [13]. This was done for both the Friedman and Vyazovkin methods.

Proximate and ultimate analyses

The American Society for Testing and Materials (ASTM) methods were used to carry out the approximate and ultimate analysis, as shown in Table 1.

The three raw coal samples (EM1, WM1 and S3-5) yielded 22.4–23.8% of volatile matter, moisture content between 3.6 and 4.3%, and ash yield between 21.7 and 23.8%. According to the results reported, Botswana coal has a high carbon content ranging from 56.4 to 60.7% and a relatively low total sulfur content ranging from 1.0 to 1.9%, indicating that the coal is classified as low sulfur content as proposed by (Chou [21]) where coal is generally termed as low sulfur (≤ 1 wt% sulfur content), medium sulfur (≥ 1 to ≤ 3 wt% sulfur content) and high sulfur coal (≥ 3 wt% sulfur content) based on their sulfur content [21]. The oxygen content O_2, was determined by subtracting the total percentage of C, H, N, S, carbonate, ash, and moisture content from one hundred per cent. The calorific value of the coal samples ranged from 21.8 to 22.6 MJ/kg, which indicates that heat is released during the complete pyrolysis process of the coal samples.

Table 1 Proximate and Ultimate analysis of Morupule coal samples [12]

	Raw Coal sample		
	WM1	S3/5	EM1
Proximate analysis (wt%)			
Moisture[a]	3.7 ± 0.2	4.3 ± 0.1	3.6 ± 0.1
Volatile matter[b]	22.4 ± 0.3	22.9 ± 0.2	23.8 ± 0.3
Fixed Carbon[c]	50.0 ± 0.4	51.2 ± 0.2	48.2 ± 0.2
Ash[d]	23.8 ± 0.3	21.7 ± 0.2	24.4 ± 0.4
Ultimate analysis (wt%)			
Carbon[e]	55.9 ± 0.3	60.7 ± 0.3	56.4 ± 0.8
Hydrogen[e]	4.0 ± 0.06	4.4 ± 0.29	4.6 ± 0.06
Nitrogen[e]	1.2 ± 0.01	1.4 ± 0.1	1.3 ± 0.1
Oxygen (by difference)	8.1 ± 0.2	8.9 ± 0.2	8.0 ± 0.6
Total sulfur[f]	1.6 ± 0.1	1.0 ± 0.1	1.9 ± 0.2
Calorific value[g] (MJ/kg)	21.8 ± 0.07	22.6 ± 0.1	22.3 ± 0.2
$A_{O/C}$	0.14	0.15	0.14

[a]AS™ D3173-11 [14]
[b]AS™ D3175-11 [15]
[c]AS™ D5142 [16]
[d]AS™ D3174-02 [17]
[e]AS™ D5373-21 [18]
[f]AS™ D4239 [19]
[g]AS™ D5865-98a [20]

Kinetic theory

The rate equation Eq. 1 can be used to describe the solid-state breakdown process.

$$\frac{d(\alpha)}{d(t)} = k(T) \cdot f(\alpha) \tag{1}$$

Here, the rate constant, $k(T)$, and the degree of conversion "α" at any time can be calculated from the mass loss information of the decomposed sample. It can be stated as: $\alpha = \frac{m_o - m_t}{m_o - m_f}$. $f(\alpha)$ is the derivative representation of the reaction model.

Here, m_o is the original sample mass in mg, m_t is the actual mass recorded at a specific time t, and m_f is the sample mass after pyrolysis.

The Arrhenius equation obtains the temperature dependence of the kinetic constant

$$k = A \exp\left(\frac{-E_a}{RT}\right) \tag{2}$$

in which: $E\alpha$ the apparent activation energy (kJ/mol), T temperature (K), R the gas constant (8.314 J/K/mol), A the frequency factor (min^{-1})

The fundamental statement of the analytical method was obtained by entering the rate constant k value in Eq. 1. The kinetic analysis that follows Eq. 3 was proposed by Piloyan et al.

$$\frac{d\alpha}{dt} = A \cdot f(\alpha) \cdot \exp\left(\frac{-E_a}{RT}\right) \tag{3}$$

We obtained Eq. 4 by taking the natural logarithm of Eq. 3.

$$\ln\left(\frac{d\alpha}{dt}\right) = \ln(A) + \ln(f(\alpha)) - \frac{-E_a}{RT} \tag{4}$$

According to Piloyan et al. the term $\ln(f(\alpha))$ could be disregarded, and the values of E and ln (A) are therefore calculated by plotting $\ln\left(\frac{d\alpha}{dt}\right)$ versus $1/T$ [22]. The error rate experienced while predicting E values has been estimated to be between 15 and 20%. However, this method has continued with the approaches that assess the kinetic triplet at a single heating rate. Similarly, Criado and Ortega came to similar findings about the limitations of their research and provided the precise computation of the inaccuracy in E brought on by this assumption [23]. According to Flynn, f (α) fluctuates in accordance with the nth power of the remaining mass fraction in a reaction model [24].

$$f(\alpha) = (1 - \alpha)^n \tag{5}$$

n is the reaction order.

By changing expression Eq. (5) to include expression Eq. (6):

$$\ln\left(\frac{d\alpha}{dt}\right) = \ln(A) + n\ln(1-\alpha) - \frac{-E_a}{RT} \tag{6}$$

For non-isothermal TGA studies with a linear ramp rate, $\beta = \frac{d\alpha}{dt}$ Eq. 6 can be reformulated.

$$\ln\left(\frac{d\alpha}{dt}\right) = \ln\left(\frac{A}{\beta}\right) + n\ln(1-\alpha) - \frac{-E_a}{RT} \tag{7}$$

The fraction of material consumed in relation to temperature is expressed by Eq. 7. Model-free techniques are utilized to estimate the kinetic parameters in non-isothermal conditions.

In this work, four different isoconversional methods and model-fitting kinetic methods were used. The TGA experiments were performed at different rates of heating of 5, 10, 15, 20, 25 °C/min to derive the basic kinetic parameters, such as the activation energy and the Arrhenius constant.

Model-free methods

Model-free approaches often report activation energies because they calculate the reaction activation energy ($E\alpha$) without making model assumptions. Iso-conversional methods are model-free approaches for evaluating kinetic variables such as activation energy ($E\alpha$) and pre-exponential factor (A) at progressive degrees of conversion α. Since they frequently include complex processes, iso-conversional approaches are essential for demonstrating solid-state kinetics. The terms "model-free" and "iso-conversational" are sometimes used interchangeably. But not all model-free approaches are isoconversional. The Kissinger method is one of these exceptions, as it does not allow calculating $E\alpha$ values with progressively higher α values and instead assumes constant apparent activation energy. Both isothermal (where the temperature varies) and non-isothermal (where the heating rate changes) data can be analysed using the isoconversional method. Several isoconversional approaches were proposed in non-isothermal kinetics in the 1960s [25–27]. A few of them are listed in the subsequent sections.

Flynn Wall Ozawa method

By plotting a graph between natural logarithms of heating rates, $\ln(\beta)$ and 1000/T, which depicts the linear relationship with a distinct conversion value at various heating rates, the FWO approach enables one to determine apparent activation energy [28].

In the FWO method, the kinetics of the reaction is described as:

$$\ln(\beta) = \ln\left(\frac{AE}{g(\alpha)R}\right) - 5.331 - 1.052\frac{E}{RT} \tag{8}$$

where T, A, R, β, and E are Temperature (K), frequency factor (min^{-1}), gas constant (8.314 J/K/mol), heating rate (°C/min), and activation energy (kJ/mol).

Kissinger Akahira Sunose

The KAS method was also applied considering the following equation, whereas the plot of $\ln \frac{\beta}{T^2}$ versus *1000/T* for a constant value of *x* should be a straight line whose slope can be used to evaluate the activation energy [29].

$$\ln \frac{\beta}{T^2} = \ln \left(\frac{AR}{g(\alpha)E} \right) - \frac{E}{RT} \tag{9}$$

In this study, only Friedman and Vyazovkin methods were applied to derive basic kinetic parameters.

Friedman

Friedman's suggested equation can be presented as:

$$\ln \left(\frac{d\alpha}{dt} \right) = \ln(Af(\alpha) - \frac{E}{RT} \tag{10}$$

The activation energy (*E*) is calculated based on the slope of the curve $\ln(dx/dt)$ with respect to 1000/*T* with a constant rate of conversion.

Vyazovkin

The activation energy value that minimizes (Eα), a function of the activation energy, can be determined using the Vyazovkin approach for a collection of temperature values acquired at the same conversion value α for *n* distinct heating rates [30].

$$\phi(E\alpha) = \sum_{i=1}^{n} \sum_{j \neq i}^{n} \frac{J[E\alpha, Ti(t\alpha)]}{J[E\alpha, Tj(t\alpha)]} \tag{11}$$

Results and discussion

Thermal behavior of coal

The results for the thermogravimetric (TG) and derivative thermogravimetric (DTG) for various heating rates are shown in Figs. 1, S1 and S2. The TG curve displays the sample's percentage mass loss across the 25–900 °C temperature range. The rate of mass loss depends on the temperature. All the peaks contained a strong peak attributed to the primary devolatilization process of coal between 350 and 550 °C. These findings correlate well with those found by Tabbiruka et al. and this process proceeds fast with an increase in temperature up to 800 °C [9]. The greater
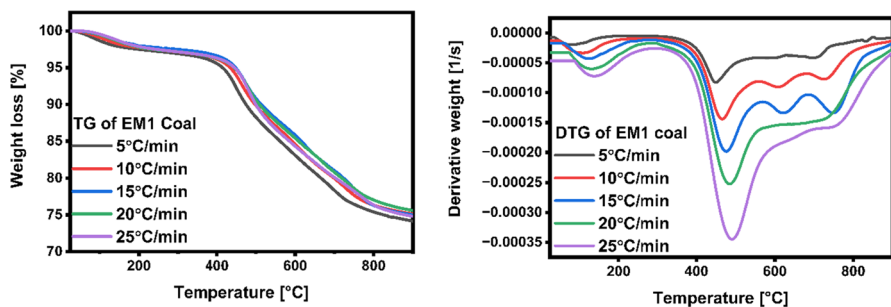
Fig. 1 TG (left) and DTG (right) of the EM1 pyrolysis at five different heating rates under an inert atmosphere

the temperature, the bigger the mass loss because the pyrolysis process is slow at low temperatures. The heating rate has no noticeable effect on the mass loss curve. Increasing the heating rate only changed the maximum temperature to a higher value, and the thermal profile of the decomposition remained unchanged. The first peak represents water release which occurs below 250 °C. The second peak corresponded to the primary decomposition phase of coal within the temperature range of 300–700 °C. This temperature range has high amount of volatile materials, which releases gaseous products such as hydrogen, carbon monoxide, carbon dioxide, and methane. This temperature range is marked by significant weight loss and complex chemical reactions, such as releasing tar and gaseous compounds and creating semi-char [31]. The last stage is observed above 700 °C where low decomposition rates occur.

Figs. 2, 3 and 4) display the conversion graph as a function of temperature at various heating rates. The kinetic curves exhibited a typical sigmoidal shape. Since a high heating rate has a shorter degradation period at the same temperature and time setting, the temperature needed for the sample to attain the exact conversion is higher as the heating rate increases. Figure 2 also represents the smoothed $\beta(d\alpha/$
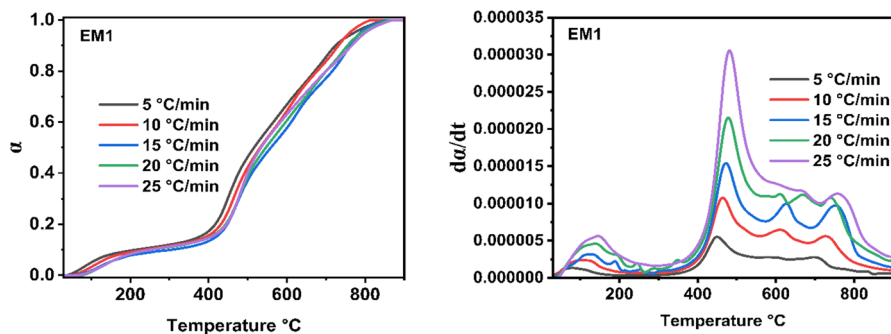

Fig. 2 Conversion (left) and smoothed derivative conversion (right) curve for pyrolysis of EM1 coal at five various heating rates under inert atmosphere
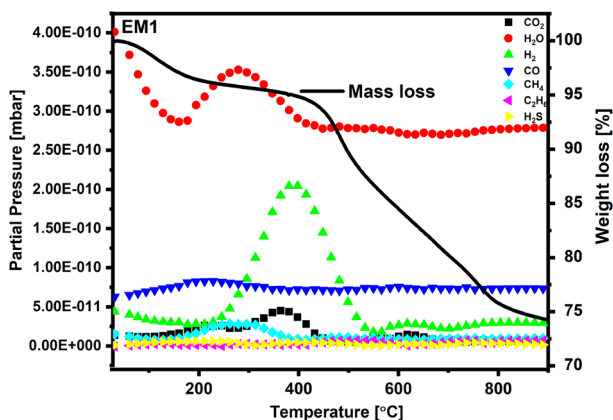
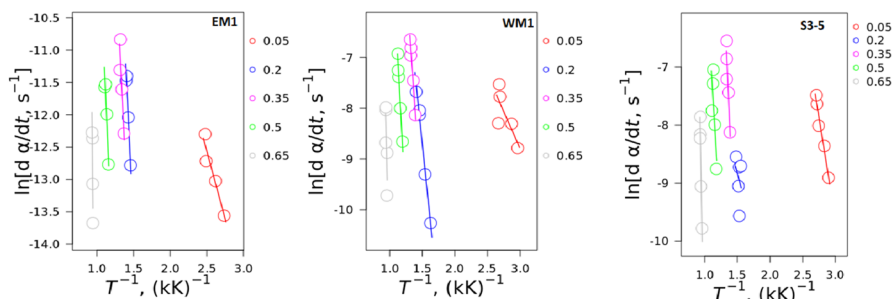**Fig. 3** Mass spectrum of gas emissions from EM1 pyrolysis

Fig. 4 Friedman graphs for the pyrolysis of Morupule coal with various conversion levels

dT) versus T curves of coal pyrolysis at 5, 10, 15, 20, and 25 °C/min heating rates. It can be observed that the peak value of the derivative increases as the heating rate increases. The temperature at the peak derivative rises with the increasing heating rate. Conversion values between 0.1 and 0.9 were taken into account when calculating kinetic parameters. Information about the derivative conversion curve peak for EM1 coal pyrolysis is provided in Table 2, while information for WM1 and S3-5 coal pyrolysis are provided in (Table S1).

TG-MS results

The mass spectrometer investigated the components of gases that escaped during pyrolysis by determining various gase's mass-to-charge ratios. Table 3 represents different chemical species that were monitored during the co-pyrolysis. According to (Figs. 3, S5 and S6), the evolved gaseous products were dominated by light volatiles like H_2 (m/z = 2) and H_2O (m/z = 18), carbon oxides like CO (m/z = 29 and CO_2 (m/z = 44) and aliphatic hydrocarbons like CH_4 (m/z = 15). The main gases emitted

Table 2 Peak Characterization of derivative conversion curve for EM1 coal pyrolysis at heating rates of 5, 10, 15, 20 and 25 °C/min

$\beta \frac{d\alpha}{dT}|T|s^{-1}$	
β/°C/min	EM1
5	5.516×10^{-6}
10	1.077×10^{-5}
15	1.539×10^{-5}
20	2.145×10^{-5}
25	3.051×10^{-5}

Table 3 Chemical species released during pyrolysis

m/z	Chemical species
2	H_2
15	CH_4
18	H_2O
27	C_2H_6
29	CO
34	H_2S
44	CO_2

during the pyrolysis process had molecular weights ranging from 2 to 64 and were at temperatures between 30 and 900 °C. A significant portion of hydrogen is emitted between 200 and 500 °C. The generated hydrogen gas is due to the greater amount of volatile substances in the coal sample. Similar kind of results were reported by pyrolysis of HSW coal (Western China) at a heating rate of 5, 10, 15 and 20 °C/min using the TG-MS technique by Bai et al. [32] and using MS & FTIR studies by authors [33, 34].

Kinetic analysis

A perfect linear relationship for all conversions considered can be found from Fig. 4. From Fig. 5, it can be observed that Eα depends on α: (1) From EM1 coal Eα gradually increases from 175 to 194 kJ/mol when α increases from 0.1 to 0.3; (2) Eα decreases to 166 and increases to 180 kJ/mol in the α range between 0.4 and 0.5 and lastly the activation energy sharply increased from 187 to 261 kJ/mol between 0.6 and 0.9 conversions. For WM1 coal Eα sharply increases from 15 to 165 kJ/mol in the α range between 0.1 and 0.3 conversions; a slight decrease was observed between 0.4 and 0.5 conversions (i.e. ranging between 154 and 152 kJ/mol). Lastly, Eα sharply increases from 163 to 266 kJ/mol in the α range between 0.6 and 0.9 conversions. Both EM1 and WM1 show a similar trend in activation energy; this is in agreement with the results found in the literature [35, 36]. Furthermore, despite some minor changes, the activation energy of EM1 and WM1 increases with conversion generally. For S3-5 coal, there was a gradual increase
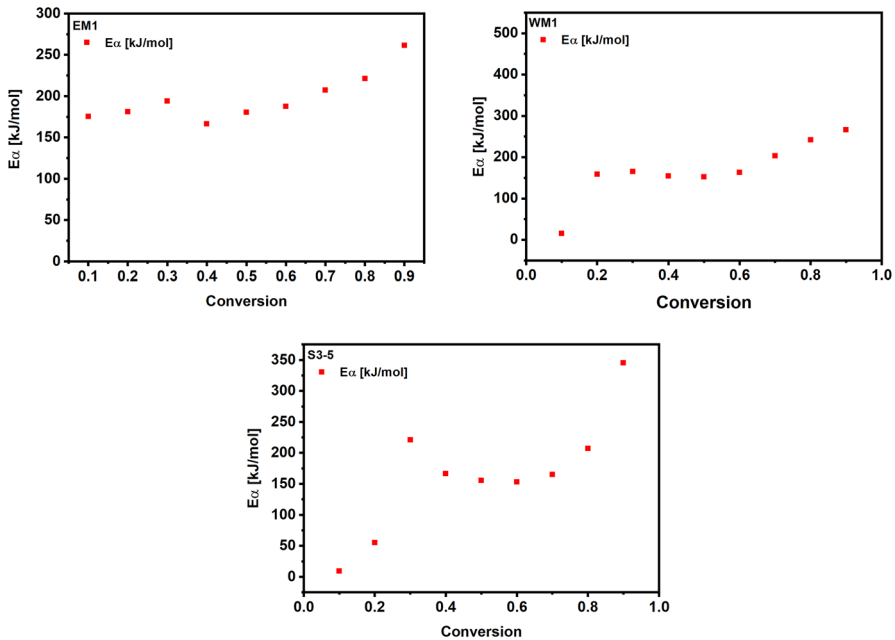
Fig. 5 Variation of the activation energy as a function of conversion for pyrolysis of EM1, WM1 and S3-5 coals at different values of conversion

of $E\alpha$ from 9 to 220 kJ/mol when α was in the range of 0.1 to 0.3; $E\alpha$ slowly decreased between 166 and 153 kJ/mol in the α range between 0.4 and 0.6, a sharp increase in activation energy occurred from 0.7 to 0.9 conversions (i.e. ranging between 164 and 345 kJ/mol). The mean activation energies calculated from Friedman methods were 164.26–197.14 kJ/mol, and the correlation coefficient factor (R^2) calculated for the three coals was between 0.7233 and 0.9165.

From Fig. 6, it can be observed that the activation energy of EM1 coal increases from a conversion of 0.1 to 0.2 (i.e., ranging between 167 and 203 kJ/mol), then decreases from 0.3 to 0.5 conversions (i.e., ranging between 190 and 153 kJ/mol), and lastly, there was a sharp increase in activation energy between conversions of 0.6–0.9 conversions (i.e., ranging between 186 and 513 kJ/mol). For WM1 coal, it can be observed that $E\alpha$ increases from 0.1 to 0.3 conversion (i.e., ranging between 10 and 157 kJ/mol), a slight decrease was observed from 0.4 to 0.5 conversions (i.e., ranging between 151 and 149 kJ/mol) and lastly, the apparent activation energy shows an increasing dependence upon the conversion degree in the range 0.6–0.9 (i.e., ranging between 160 and 496 kJ/mol). A sharp increase is observed from 0.1 to 0.3 conversions (i.e., ranging between 10 and 209 kJ/mol) for S3-5 coal. $E\alpha$ further decreased from 0.4 to 0.7 conversions (i.e., ranging between 176 and 137 kJ/mol) and $E\alpha$ slowly increased from 0.8 to 0.9 conversions (i.e., ranging between 229 and 280 kJ/mol). The mean activation
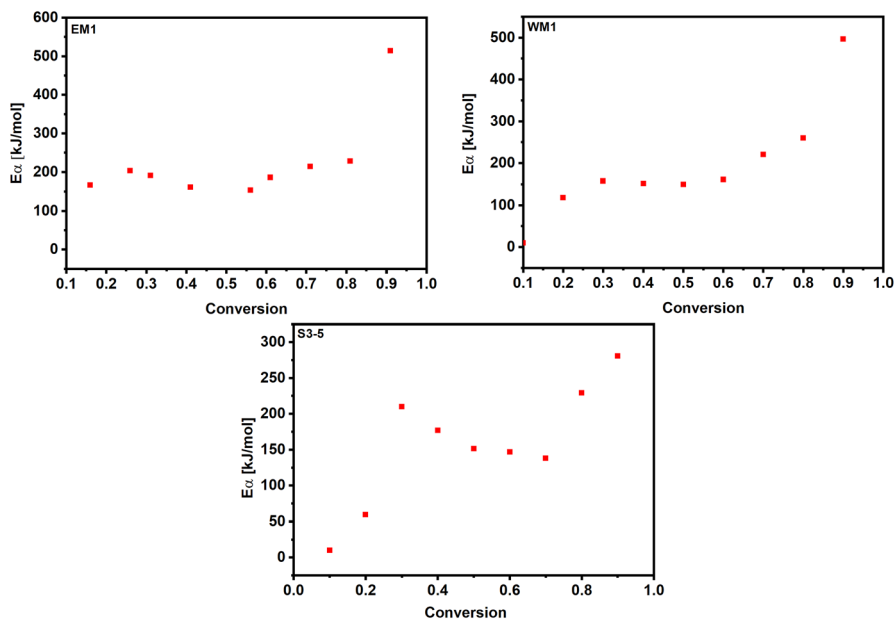
Fig. 6 The activation energy in relation to conversion using the advanced integral Vyazovkin method for EM1, WM1 and S3-5 coal

Table 4 Calculated kinetic parameters by the Friedman method for pyrolysis of EM1, WM1 and S3-5 coals

EM1			WM1		S3-5	
α	Eα [kJ/mol]	R^2	Eα [kJ/mol]	R^2	Eα [kJ/mol]	R^2
0.1	175.27	0.9324	15.61	0.90251	9.29	0.69779
0.2	181.00	0.96395	158.82	0.98935	55.37	0.63013
0.3	194.05	0.95338	165.32	0.97648	220.79	0.92001
0.4	166.30	0.73182	154.30	0.97382	166.54	0.63521
0.5	180.39	0.7091	152.70	0.94381	155.72	0.71467
0.6	187.50	0.75641	163.27	0.96786	153.29	0.63077
0.7	207.10	0.88942	203.19	0.95182	164.93	0.57215
0.8	221.22	0.64359	242.11	0.79861	207.22	0.80935
0.9	261.47	0.88589	266.40	0.84592	345.15	0.89929
Average	**197.14**	**0.8168**	**169.08**	**0.9165**	**164.26**	**0.7233**

energy calculated from the advanced integral Vyazovkin method was 155–224 kJ/mol for the three coals. Tables 4 and 5 show that the two isoconversional models had very small differences in activation energy values, which ensured their validity.

Table 5 Activation energy values of coal samples by advanced integral Vyazovkin method

EM1		WM1	S3-5
α	Eα [kJ/mol]	Eα [kJ/mol]	Eα [kJ/mol]
0.1	167.17	10.00	10.00
0.2	203.62	117.83	59.41
0.3	190.78	157.33	209.86
0.4	161.50	151.31	176.67
0.5	153.98	149.80	151.41
0.6	186.43	160.70	146.73
0.7	214.30	220.33	137.96
0.8	227.88	259.72	229.24
0.9	513.90	496.41	280.61
Average	**224.40**	**191.49**	**155.77**

Conclusion

The pyrolysis of Morupule coal was performed using TGA/DSC3 + at five different rates of heating of 5, 10, 15, 20 and 25 °C/min under an inert atmosphere. The Friedman and the advanced integral Vyazovkin methods were applied to the TGA data to calculate the kinetic parameters. The influence of the heating rate on coal pyrolysis was also investigated. The heating rate affected the main pyrolysis process at temperatures ranging from 300 to 700 °C. From the experiments, it was found that with higher heating rates, the rate of coal thermal decomposition was increasing. The Arrhenius parameters from Friedman and advanced integral Vyazovkin showed a similar trend in the activation energy of the three coals. However, the advanced integral Vyazovkin method, which makes use of more precise approximations, was figured to be more appropriate. The mean activation energy calculated from the advanced integral Vyazovkin method was 155–224 kJ/mol. For the three types of coal, the gas formation process during pyrolysis is essentially the same. According to intensity distribution H_2 and H_2O dominated the evolved gaseous products, while CO, CO_2 and CH_4 were the lesser products. More significant amounts of hydrogen and carbon monoxide can be used to produce synthesis gas (syngas). Researchers and the coal industry can better understand coal pyrolysis and gasification dynamics and optimize process conditions using the kinetic parameters discovered in this work.

Declarations

Conflict of interest The authors have no competing interests to declare relevant to this article's content.

References

1. Wheeldon JM et al (2008) Energy resources, conversion and utilization. McGraw hill, New York
2. Cloke M, Wu T, Barranco R, Lester E (2003) Char characterisation and its application in a coal burnout model. Fuel 82:1989–2000
3. World coal Institute-2007
4. Baruya PK (2013) Coal prospects in Botswana, Mozambique, Zambia, Zimbabwe and Namibia. IEA Clean Coal Centre 20:103–115
5. Agarwal A, Dintwa E (2016) Assessment of energy demand and supply framework IN Botswana. Int J Eng Res Gen Sci 4:1–9
6. Campoy M, Gómez-Barea A, Vidal FB, Ollero P (2009) Air-steam gasification of biomass in a fluidised bed: process optimisation by enriched air. Fuel Process Technol 90:677–685. https://doi.org/10.1016/j.fuproc.2008.12.007
7. Keboletse KP, Mongalenyane T, Kelebopile L et al (2018) Investigating the suitability of morupule coal for coal gasification technology. MRS Adv Mater Res Soc 3:2235–2245
8. Bikane K, Yu J, Shankar R et al (2021) Early-stage kinetics and char structural evolution during CO_2 gasification of Morupule coal in a wire-mesh reactor. Chem Eng J. https://doi.org/10.1016/j.cej.2020.127803
9. Nadiye-Tabbiruka MS (2014) Thermal-gravimetric, calorimetric and chemical analytical characterisation of coal. Int J Mater Sci Appl 3:325. https://doi.org/10.11648/j.ijmsa.20140306.18
10. Xu Y, Zhang Y, Wang Y et al (2013) Thermogravimetric study of the kinetics and characteristics of the pyrolysis of lignite. React Kinet Mech Catal 110:225–235. https://doi.org/10.1007/s11144-013-0586-x
11. Matsuoka K, Akiho H, Xu WC et al (2005) The physical character of coal char formed during rapid pyrolysis at high pressure. Fuel 84:63–69. https://doi.org/10.1016/j.fuel.2004.07.006
12. Nermark FM (2022) Application of subcritical and supercritical fluids in coal extraction and analysis. Lund University, Lund
13. Muravyev NV, Pivkina AN, Koga N (2019) Critical appraisal of kinetic calculation methods applied to overlapping multistep reactions. Molecules. https://doi.org/10.3390/molecules24122298
14. ASTM International (2017) D3173/D3173M standard test method for moisture in the analysis sample of coal and coke. https://www.astm.org/d3173_d3173m-17a.html. Accessed 21 Jul 2023
15. ASTM International (2011) Test method for volatile matter in the analysis sample of coal and coke. https://scholar.google.com/scholar?hl=en&as_sdt=0%2C5&q=+Standard+Test+Method+for+Volatile+Matter+in+the+Analysis+Sample+of+Coal+and+Coke%2C+West+Conshohocken&btnG=. Accessed 21 Jul 2023
16. ASTM International (2013) Standard practice for proximate analysis of coal and coke. https://scholar.google.com/scholar?hl=en&as_sdt=0%2C5&q=ASTM+International+%282013%29%2C+ASTM+D5142+Standard+Practice+for+Proximate+Analysis+of+Coal+and+Coke+1.+&btnG=. Accessed 21 Jul 2023
17. AMST (2004) Standard test method for ash in the analysis sample of coal and coke from coal. https://scholar.google.com/scholar?hl=en&as_sdt=0%2C5&q=Standard+Test+Method+for+Ash+in+the+Analysis+Sample+of+Coal+and+Coke+from+Coal%2C+ASTM+International%2C+West+Conshohocken%2C+PA%2C+2002.&btnG=. Accessed 21 Jul 2023
18. ASTM International (2014) Standard test methods for determination of carbon, hydrogen and nitrogen in analysis samples of coal and carbon in analysis samples of coal and coke. https://scholar.google.com/scholar?hl=en&as_sdt=0%2C5&q=ASTM+International+%282014%29%2C+ASTM+D5373+-+21+Standard+Test+Methods+for+Determination+of+Carbon%2C+Hydrogen+and+Nitrogen+in+Analysis+Samples+of+Coal+and+Carbon+in+Analysis+Samples+of+Coal+and+Coke.+&btnG=. Accessed 21 Jul 2023
19. ASTM International (2008) D4239. Standard test methods for sulfur in the analysis sample of coal and coke using high-temperature tube furnace combustion methods. https://scholar.google.com/scholar?hl=en&as_sdt=0%2C5&q=ASTM+International+%282008%29%2C+ASTM+D4239+Standard+test+methods+for+sulfur+in+the+analysis+sample+of+coal+and+coke+using+high-temperature+tube+furnace+combustion+methods.+&btnG=. Accessed 21 Jul 2023
20. ASTM International (2007) A standard test method for gross calorific value of coal and coke. https://scholar.google.com/scholar?hl=en&as_sdt=0%2C5&q=ASTM+International+%282007%

29%2C+ASTM+D5865-98a+A+standard+test+method+for+gross+calorific+value+of+coal+and+coke.++&btnG=. Accessed 21 Jul 2023
21. Chou CL (2012) Sulfur in coals: a review of geochemistry and origins. Int J Coal Geol 100:1–13
22. Woods GS (1963) Chemistry determination of activation energies of chemical reactions by differential thermal analysis. Pergamon Press, Oxford
23. Criado JM, Ortega A (1984) Errors in the determination of activation energies of solid-state reactions by the piloyan method, as a function of the reaction mechanism. J Therm Anal 29:1075
24. Flynn JH (1991) A general differential technique for the determination of parameters for d (α)/dt= f (α) A exp (− E/RT) energy of activation, preexponential factor and order of reaction (when applicable). J Therm Anal Calorim 37(2):293–305
25. Friedman HL (1964) Kinetics of thermal degradation of char-forming plastics from thermogravimetry. Application to a phenolic plastic. J Polym Sci Part C Polym Symp 6:183
26. Ozawa T (1965) A new method of analyzing thermogravimetric data. Bull Chem Soc Jpn 38:1881
27. Flynn JH, Wall LA (1966) A quick, direct method for the determination of activation energy from thermogravimetric data. J Polym Sci B 4:323–328. https://doi.org/10.1002/POL.1966.110040504
28. Flynn JH, Wall LA (1966) General treatment of the thermogravimetry of polymers. J Res Natl Bur Stand Sect Phys Chem 70(6):487
29. Akahira T (1971) Trans. Joint convention of four electrical institutes. Res Rep Chiba Inst Technol. 16:22–31
30. Khawam A (2007) Application of solid-state kinetics to desolvation reactions. The University of Iowa, Iowa
31. Sharma S, Ghoshal AK (2010) Study of kinetics of co-pyrolysis of coal and waste LDPE blends under argon atmosphere. Fuel 89:3943–3951. https://doi.org/10.1016/j.fuel.2010.06.033
32. Bai H, Mao N, Wang R et al (2021) Kinetic characteristics and reactive behaviors of HSW vitrinite coal pyrolysis: a comprehensive analysis based on TG-MS experiments, kinetics models and ReaxFF MD simulations. Energy Rep 7:1416–1435. https://doi.org/10.1016/j.egyr.2021.09.100
33. Zhou B, Shi L, Liu Q, Liu Z (2016) Examination of structural models and bonding characteristics of coals. Fuel 184:799–807. https://doi.org/10.1016/j.fuel.2016.07.081
34. Wang YG, Wei XY, Wang SK et al (2016) Structural evaluation of Xiaolongtan lignite by direct characterization and pyrolytic analysis. Fuel Process Technol 144:248–254. https://doi.org/10.1016/j.fuproc.2015.12.034
35. Yan J, Jiao H, Li Z et al (2019) Kinetic analysis and modeling of coal pyrolysis with model-free methods. Fuel 241:382–391. https://doi.org/10.1016/j.fuel.2018.12.079
36. Yan J, Yang Q, Zhang L et al (2020) Investigation of kinetic and thermodynamic parameters of coal pyrolysis with model-free fitting methods. Carbon Resour. Convers 3:173–181. https://doi.org/10.1016/j.crcon.2020.11.002

Authors and Affiliations

Kgalalelo P. Kgatlane[1,2] · Sebusi Odisitse[1] · Casper Gate[3] · James Darkwa[2,4] · Isaac N. Beas[2,5]

✉ Isaac N. Beas
ibeas@bitri.co.bw

Kgalalelo P. Kgatlane
pkgatlane@bitri.co.bw

Sebusi Odisitse
odisitses@biust.ac.bw

Casper Gate
gatecasp@msu.edu

James Darkwa
jdarkwa@bitri.co.bw

1   Department of Chemical and Forensic Sciences, Botswana International University of Science and Technology, Palapye, Botswana

2   Department of Natural Resources and Materials, Botswana Institute for Technology Research and Innovation, Maranyane House, Plot 50654 Machel Drive, Gaborone, Botswana

3   Department of Chemical Engineering and Materials Science, Michigan State University, 428 S Shaw Ln, East Lansing, MI 48824, USA

4   Department of Chemistry, University of Johannesburg, PO Box 524, Auckland Park Kingsway Campus 2006, South Africa

5   Department of Chemical Engineering, University of South Africa, P/Bag X6, Florida, Johannesburg 1710, South Africa